Journal of Advanced Marine Engineering and Technology, Vol. 45, No. 6, pp. 339~344, 2021
J. Advanced Marine Engineering and Technology (JAMET)
https://doi.org/10.5916/jamet.2021.45.6.339
ISSN 2234-7925 (Print)
ISSN 2765-4796 (Online)
Original Paper

Study on the fundamental thermal analysis of thermoelectric generator systems

JikSu Yu[1] · MyoungJun Kim†

(Received July 17, 2021 ; Revised July 21, 2021 ; Accepted November 29, 2021)

Abstract: This study investigates the temperature characteristics and efficiency of a Peltier element for waste heat recovery from a ship. The Peltier element is calculated using its heat balance and performance. The results are as follows: 1) In the case of gas and water as the heat source, the temperature profile estimated from the performance and heat balance of the Peltier element generated deviations. 2) In the case of gas and water as the heat source, the thermoelectric scale effect changed the heat transfer rate considered between the heat source and the Peltier element existed. 3) In the case of water as the heat source, the thermoelectric scale effect changed the heat transfer rate considered between the heat source and the Peltier element did not exist.

Keywords: Waste heat, Thermoelectric generation, Peltier element, Scale effect, Heat transfer rate

1. Introduction

The world is making various efforts to reduce greenhouse gas (GHG) emissions, the main culprits of global warming. The Republic of Korea, the world's seventh largest emitter of GHGs, aims to reduce GHG emissions by 37 % compared to "business as usual" by 2030 according to the Paris Climate Agreement. Measures such as the conversion from fossil fuels to new and renewable energies are being considered as a way to reduce GHG emissions. However, efforts in each industry and alternative energy resources to existing fossil fuels are required to achieve the 2030 GHG emissions reduction goal.

Recently, research on energy conversion has been conducted to recover renewable energy, such as waste heat, from industrial processes. Among the research on energy conversion, thermoelectric power generation using the Peltier element is being studied because this element is small and simple. Moreover, research related to thermoelectric power generation is actively being conducted **[1][2]**.

Thermoelectric power generation generates electricity from heat using the "Seebeck effect," which generates a voltage when there is a temperature difference between two different types of metals or semiconductors, and directly recovers waste heat as electrical energy without using other fossil fuels. It is a material technology that best responds to GHG reduction policies through energy saving **[3]**. Thermoelectric device technology is widely applied in automobiles, aerospace/aviation, semiconductors, optics, computers, power generation, and home appliances **[4][5][6]**. To apply these technologies to various fields and increase the efficiency of the systems, research is being conducted in research institutes and companies; however, research applied to ships is insufficient.

The purpose of this study is to incorporate a thermoelectric power generation system on a ship to recover the waste heat given off as exhaust gas from the ship. In addition, we intend to understand the temperature distribution and efficiency inside the system by considering the heat balance between the heat source and the thermoelectric element. Calculations are performed using MathCad Prime 3.0 in the engineering tools.

2. Heat Source and Thermoelectric Element Specifications of Calculation Model

Table 1 lists the conditions of the heat source, and **Table 2** lists the specifications of the thermoelectric element. To simplify the analysis, it is assumed that the properties of the Peltier element do not depend on temperature.

Figure 1 shows the thermal analysis model. The heat balance between the Peltier element and the heat source is calculated following the procedure detailed by the conventional research of

† Corresponding Author (ORCID: http://orcid.org/0000-0002-9498-5503): Professor, Division of Marine Engineering, Kunsan National University, 558, Daehak-ro, Gunsan-si, Jeollabuk-do 54150, Korea, E-mail: mjkim@kunsan.ac.kr, Tel: +82-63-469-1849
1 Ph. D., Head Office of Kunsan University, Kunsan Natioinal University, E-mail: jiksuyu@kunsan.ac.kr, Tel: +82-63-469-8990

Table 1: Heat source samples of thermoelectric generator system

Define of heat source	At the hot side		At the cold side
Heat transfer medium	Exhaust gas	Used coolant of lubricant	Coolant
Temperature, °C	300	80	20
Mechanism of heat transfer	Forced Convection		
Film coefficient of heat transfer, W/m^{2}K	50	6,000	6,000
Quality of plumbing	Stainless		
Thickness of plumbing, m	0.01		
Thermal conductivity, W/mK	16.5		
Overall heat transfer coefficient, W/m^{2}K	48.5	1,290	1,290

Table 2: Specifications of Peltier element

Country of Manufacture		Japan
Maker		Kyocera
Model No.		40×40 Module
Item	Unit	Value
Length	mm	40
Width	mm	40
Area, S	mm^2	1600
Thickness	mm	2.3
Temperature at the hot side, T_{hj}	℃	20
Temperature difference, ΔT_j	℃	67
Temperature at the cold side, T_{cj}	℃	-47
Average temperature, $(T_{hj} + T_{cj})/2$	℃	-13.5
Seebeck coefficient, α	V/K	4.836×10^{-3}
Internal resistance, R_i	Ω	1.900
Internal resistance rate, ρ_i	Ωm	1.322
Internal heat conductance, K	W/K	4.908×10^{-3}
Internal thermal conductivity, λ_i	W/mK	7.055×10^{-3}
Thermoelectric figure of merit, Z	1/K	2.508×10^{-3}

Table 3: Peltier element arrangement

Module	Unit	Single	Serial	Parallel	Serial+Parallel
Number	ea	1	m	n	m×n
Seebeck coefficient	W/K	α	mα	α	mα
Interal resistance	Ω	R	mR	R/n	(m/n)R
Heat conductance	W/K	K	mK	nK	mnK

an author **[7]** as follows:

① Calculate the intermediate temperature $T_{av}(=[T_H+T_C])/2$ between the heat sources and assume that this is the same as the intermediate temperature between the high-temperature side and the low-temperature side of the Peltier element.

② In the Peltier element, the temperature difference "T_{hj}–T_{cj}" is used as a parameter, and the initial calculated values of the high-temperature side temperature T_{hj} and the low-temperature side temperature T_{cj} of the Peltier element are obtained.

③ Set the number and arrangement of modules used in the system, and obtain the current I in the entire system from **Table 2** and ②. Regarding the module arrangement, **Table 3** shows the calculation methods according to the case of arranged in series and arranged in parallel. Additionally, the circuit diagram of the thermoelectric element is shown in **Figure 2**, and the external resistance R_o is estimated from $R_o = M_0R$, where the conversion efficiency is maximized. M_0 is calculated using **Equation (1)**.

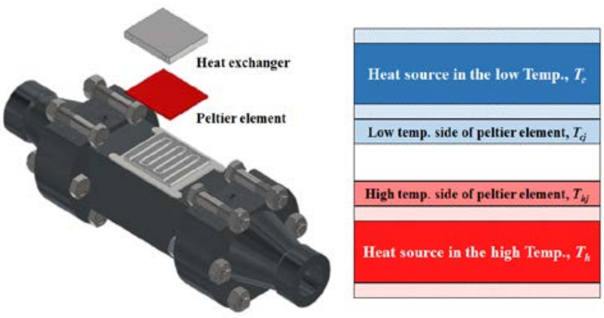

Figure 1: Thermal analysis model of the thermoelectric generator system

Table 4: Analysis condition

	CASE 1	CASE 2	CASE 3	CASE 4
Connection	Serial		Serial × Parallel	
Number of devices	4		16(4×4)	
Heat source at high temperature	Exhaust gas	Cooling water from the low temperature part	Exhaust gas	Cooling water from the low temperature part

$$M_0 = \sqrt{1 + \frac{Z(T_{hj}+T_{cj})}{2}} = \sqrt{1 + ZT_{av}} \quad (1)$$

The current I is calculated from the electromotive force V, as shown in **Equation (2)**.

$$\mathrm{I} = \frac{V}{R+R_0} = \frac{\alpha(T_{hj}-T_{cj})}{(1+M_0)R} \quad (2)$$

④ In this analysis, two types are set: four in series and four in series × four in parallel to prove the effect of heat transfer.

⑤ The energy balance at the high- and low-temperature sides of the thermoelectric module is shown by **Equations (3)** and **(4)**, respectively.

$$Q_h = K(T_h - T_{hj}) + \alpha T_{hj} I - 0.5 I^2 R \quad (3)$$

$$Q_c = K(T_{cj} - T_c) + \alpha T_{cj} I - 0.5 I^2 R \quad (4)$$

⑥ The temperature difference between the high- and low-temperature sides of the thermoelectric element can be obtained using **Equation (5)**.

$$T_{hj} - T_{cj} = \frac{(T_h - T_c) - \frac{\alpha I}{S}\left(\frac{T_h}{U_h} - \frac{T_c}{U_c}\right) + \frac{0.5RI^2}{S}\left(\frac{1}{U_h} - \frac{1}{U_c}\right) - \frac{\alpha R I^3}{U_h U_c S^2}}{1 + \frac{K}{S}\left(\frac{1}{U_h} + \frac{1}{U_c}\right) + \frac{\alpha I}{S}\left(\frac{1}{U_h} - \frac{1}{U_c}\right) - \frac{1}{U_h U_c}\left(\frac{\alpha I}{S}\right)^2} \quad (5)$$

⑦ **Equation (6)** is calculated from the heat balance on the high-temperature side of the thermoelectric element.

$$T_{h,j} = \frac{F_2 T_c + F_3 T_h + F_4}{F_1} \quad (6)$$

Here, the coefficients F_1, F_2, F_3, and F_4 in **Equation (6)** are obtained using the following equations:

$$F_1 = 1 + \frac{K}{S}\left(\frac{1}{U_h} + \frac{1}{U_o}\right) + \frac{\alpha I}{S}\left(\frac{1}{U_h} - \frac{1}{U_o}\right) - \frac{1}{U_h U_o}\left(\frac{\alpha I}{S}\right)^2$$

$$F_2 = \frac{K}{U_h S}$$

$$F_3 = \frac{0.5RI^2}{U_h S} + \frac{K - 0.5\alpha I}{U_h U_o S^2} R I^2$$

⑧ **Equation (7)** is calculated from the heat balance of the low-temperature side in the thermoelectric element.

$$T_{cj} = \frac{F_5 T_c + F_6 T_h + F_7}{F_1} \quad (7)$$

Here, the coefficients F_5, F_6, and F_7 are obtained by the following equations:

$$F_5 = \left(1 + \frac{K + \alpha I}{U_h S}\right)$$

$$F_6 = \frac{K}{U_o S}$$

$$F_7 = \frac{0.5RI^2}{U_o S} + \frac{K + 0.5\alpha I}{U_h U_o S^2} R I^2$$

⑨ For each parameter, the value obtained in **Equation (5)** is compared with the values obtained by **Equations (6)** and **(7)**, and the parameter with a small error is set as a reasonable value.

⑩ The conversion efficiency η in the system is calculated by **Equation (8)**.

$$\eta_T = \frac{T_{hj} - T_{cj}}{T_{hj}}, \ \eta = \frac{\eta_T (M_0 - 1)}{M_0 + \frac{T_{cj}}{T_{hj}}} \quad (8)$$

4. Calculation results

4.1 CASE 1: Exhaust gas is used as a heat source on the high-temperature side (arrangement of four thermoelectric elements in series).

The analysis results for CASE 1 are shown in **Figure 3**. The result of the performance of the Peltier element is the initial calculated value obtained in ② of Section 3, and the result of the heat balance shows the value calculated over ⑦ to ⑨ of Section 3.

When checking the temperature difference between the heat source and the thermoelectric element from the value calculated by the heat balance, it can be seen that a difference of 0.61 °C on the low-temperature side and of 47.17 °C on the high-temperature side occurred. The reason for this temperature difference was considered to affect the temperature distribution by a phenomenon in which the overall heat transfer coefficient on the high-temperature side is significantly lower than the value on the low-temperature side.

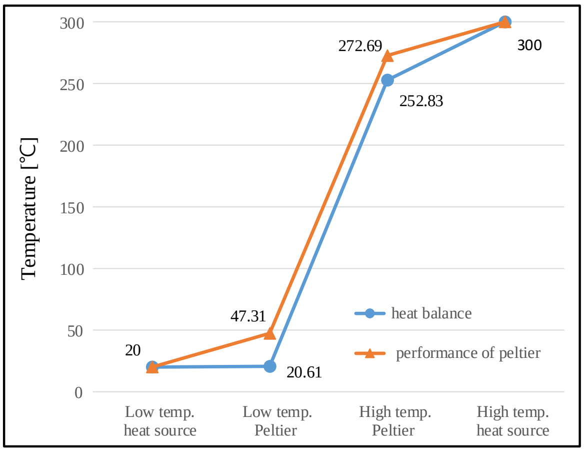

Figure 3: (CASE 1) Temperature profiles of the thermoelectric generator system

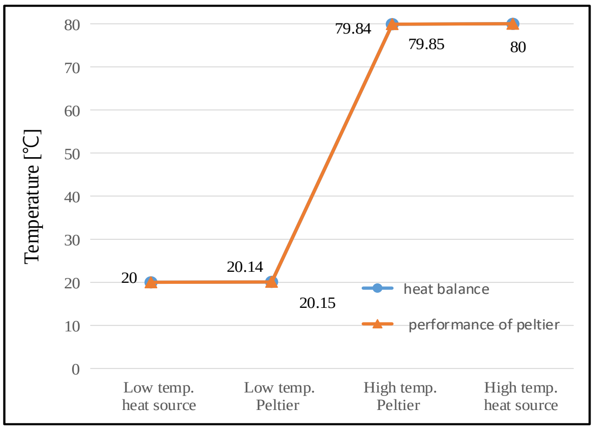

Figure 4: **(**CASE 2) Temperature profiles of the thermoelectric generator system

4.2 CASE 2: The coolant that has already completed the heat exchange on the low-temperature side is reused as a heat source on the high-temperature side (arrangement of four thermoelectric elements in series).

The analysis results for CASE 2 are shown in **Figure 4**. Unlike CASE 1, it can be seen that the temperature difference between the thermoelectric element and the heat source did not occur in both the high- and low-temperature sides. This result indicated that the total heat transfer coefficient of the high-temperature side increased to a greater extent than that of CASE 1, and there was little difference in the total heat transfer coefficient of the low-temperature side.

4.3 CASE 3: Exhaust gas is used as a heat source on the high-temperature side (arrangement of four thermoelectric elements in series × four thermoelectric elements in parallel: total 16).

To confirm the effect of increasing the scale of the system, a calculation was performed when the number of thermoelectric elements was increased from four to 16 (four in series × four in parallel) without changing the heat source under the condition of CASE 1.

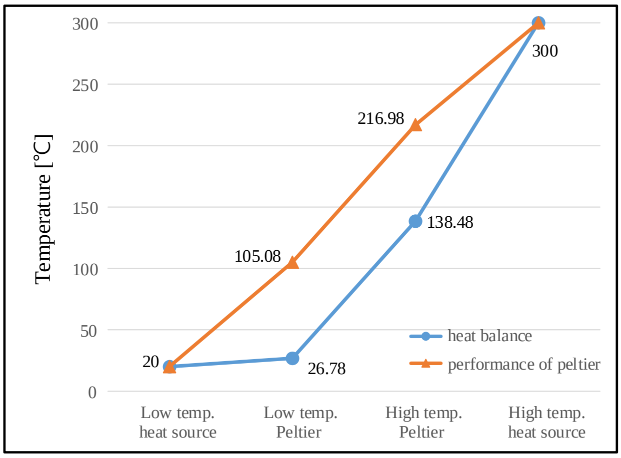

Figure 5: (CASE 3) Temperature profiles of the thermoelectric generator system

The results are shown in **Figure 5**.

Compared to the results of CASE 1, the results of the Peltier element performance showed that the temperature difference between the thermoelectric elements changed from ~200 °C to ~110 °C. In addition, as a result of the heat balance, it was confirmed that the temperature difference between the thermoelectric elements decreased from ~200 °C to ~110 °C.

Looking at the result calculated from the heat balance, the temperature difference between the heat source and the thermoelectric element was ~6.8 °C on the low-temperature side and ~161.5 °C on the high-temperature side. That is, by increasing the thermoelectric element, the temperature difference between the heat source and the thermoelectric element on the low-temperature side decreased, while the temperature difference between the heat source and the thermoelectric element on the high-temperature side increased. Notably, the difference in the overall heat transfer coefficient affected the temperature distribution.

In general, the thermoelectric conversion system is widely known because one of its advantages is that it does not affect scale-up/down. In this case, it can be considered that the effect of scale-up existed owing to the influence of the overall heat transfer coefficient of the high- and low-temperature sides.

4.4 CASE 4: The coolant that has been heat-exchanged on the low-temperature side is reused as a heat source on the high-temperature side (arrangement of four thermoelectric elements in series × four thermoelectric element parallel arrangements: total 16).

Under the same conditions as in CASE 2, the result of the calculation by increasing the number of thermoelectric elements from four to 16 (four in series × four in parallel) without changing the heat source is shown in **Figure 6**.

Comparing the results of CASES 4 and 2, it can be seen that the temperature distribution and temperature at each point were almost the same. From this result, it can be considered that there was little effect of increasing the number of thermoelectric elements. This was considered to be because the overall heat transfer coefficient on the high-temperature side and the cooling side was sufficiently high.

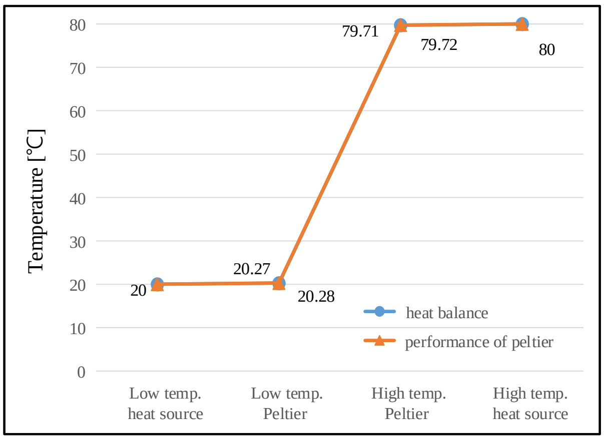

Figure 6: (CASE 4) Temperature profiles of the thermoelectric generator system

4.5 Maximum efficiency of thermoelectric generator system

Figure 7 shows the system efficiency of each CASE. First, if we check the results calculated with the heat balances of CASES 1 and 3, the efficiency was approximately 9–7 %.

However, it should be noted that the voltage or current of the thermoelectric element in this case was calculated using the values from the performance of the Peltier element. The efficiency in this case was 4–8 %.

The maximum efficiency of CASES 2 and 4, where both the hot and cold heat sources were liquid, was ~2.7 %. Because the overall heat transfer coefficient was sufficiently high on the high-temperature side and the cooling side, it can be seen that the temperature distribution or efficiency did not change significantly even if the scale of the thermoelectric generator system was increased.

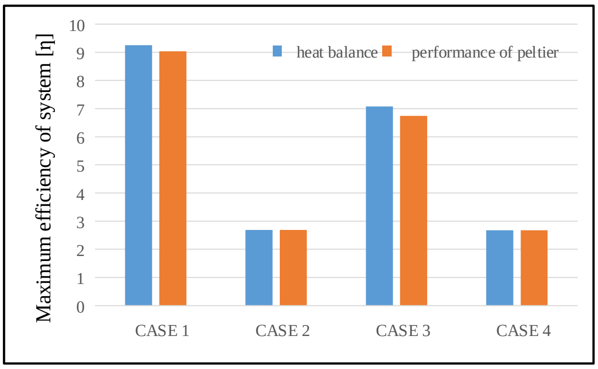

Figure 7: Maximum efficiency of the thermoelectric generator system

Meanwhile, for CASES 1 and 3, the efficiency was expected to increase further by increasing the overall heat transfer coefficient of the exhaust gas side. However, because this was related to the pressure loss of the exhaust gas side, more reviews are expected.

5. Conclusion

In this study, to introduce a thermoelectric power generation system in a ship, the following results were derived by setting the specifications of the heat source and thermoelectric element, and estimating the temperature distribution inside the system considering the heat balance between the heat source and thermoelectric element.

1. When one of the heat source media was a gas and the other a liquid, there was a deviation between the temperature distribution data estimated from the Peltier element performance and the temperature distribution data considered

from the heat balance. To reduce this deviation, it is important to accurately calculate the high- and low-temperature side temperatures of the thermoelectric element to evaluate the Peltier element performance, including the difference in the overall heat transfer coefficient.

2. As in CASES 1 and 3, when the medium of the heat source was a gas on one side and a liquid on the other side, considering the heat transfer rate between the heat source and the thermoelectric element, there was an effect of increasing the number of thermoelectric elements. This is because the overall heat transfer coefficient of the gas, which was the heat source on the high-temperature side, was very low compared to the value of the liquid.
3. In addition, when the heat source medium was liquid, the effect hardly occurred even if the number of thermoelectric elements was increased. This is because the overall heat transfer coefficient at the high-temperature side and cooling side was sufficiently high.

Acknowledgement

The author wishes to acknowledge the financial support of the Fisheries Science Institute of Kunsan National University

Author Contributions

Conceptualization, J. S. Yu and M. J. Kim; Methodology, J. S. Yu; Software, J. S. Yu; Validation, J. S. Yu and M. J. Kim; Formal Analysis, J. S. Yu; Investigation, J. S. Yu; Resources, J. S. Yu; Data Curation, J. S. Yu; Writing—Original Draft Preparation, J. S. Yu; Writing—Review & Editing, M. J. Kim; Visualization, J. S. Yu; Supervision, M. J. Kim; Project Administration, M. J. Kim; Funding Acquisition, M. J. Kim.

References

[1] S. H. Park, J. K. Lee, Y. H. Kwon and Y. C. Ahn, “Performance evaluation of ice production utilizing the thermoelectric module for the residential refrigerators,” Journal of the Korean Society for Power System Engineering, vol. 23, no. 4, pp. 5-13, 2019 (in Korean).

[2] S. H. Kim, “A study on the application of thermoelectric module in the air conditioner system using automotive,” Journal of the Korean Society for Power System Engineering, vol. 12, no. 4, pp. 32-38, 2008 (in Korean).

[3] M. J. Kim, “Study on the adsorption and desorption enhance effect of oyster shell using Peltier element,” Journal of The Korea Society for Power System Engineering, vol. 17, no. 1, pp. 71-76, 2013 (in Korean).

[4] S. Lee and S. S. Oh, “Technology trends of thermo-electric generator system for waste heat recovery,” Journal of the korea society of automotive engineers, vol. 32, no. 5, pp. 43-51, 2010 (in Korean).

[5] T. Furue, et al., “Case study on thermoelectric generation system utilizing the exhaust gas of internal combustion power plant,” Proceedings of the 17th International Conference on Thermoelectric (ICT98), Nagoya, pp. 473-478, 1998.

[6] D. M. Rowe and G. Min, “Evaluation of thermoelectric modules for power generation,” Journal of power sources, vol. 73, no. 2, pp. 193-198, 1998.

[7] M. J. Kim, G. J. Ga, G. H. Chea, and I. S. Kim, “Fundamental heat analysis about the thermoelectric generation system using the waste heat of exhaust gas from ship,” Journal of the Korea Society of Marin Environment & Safety, vol. 22, no. 5, pp. 583-592, 2016.